JOURNAL OF MATERIALS SCIENCE 32 (1997) 357–364

Microstructural development in copper-interlayer transient liquid phase bonds between martensitic NiAl and NiTi

W. F. GALE, Y. GUAN
Materials Research and Education Center, Auburn University Auburn, AL 36849, USA

Transient liquid phase (TLP) bonding of Ni–24 at % Al–16 at %Cr and Ni–30 at % Al with a tetragonal $L1_0$ type martensitic microstructure to nominally stoichiometric NiTi with a monoclinic (distorted B19 type) martensitic matrix is investigated in this paper. The TLP bonds described in this article employed 50 μm thick copper interlayers. Bonds were prepared using holding times of between 20 min and 2 h at a bonding temperature of 1150 °C. A holding time of 1 h at 1150 °C was sufficient to remove the liquid-phase from the bond-line, however a layer of Ni_2AlTi ($L2_1$ type Heusler phase) was left at the bond line. This layer remained present with further holding up to 2 h at 1150 °C. With 50 μm thick copper interlayers, 2 h holding at 1150 °C resulted in significant titanium diffusion, from the NiTi substrate, to the joint. Depletion of titanium from the NiTi substrate, in turn, reduced the solidus temperature of the NiTi substrate to the point where localized melting occurred on the surface of the NiTi substrate. Extensive microstructural changes were observed in the NiTi substrate after TLP bonding and these are discussed in detail. In contrast, the NiAl substrate was largely unchanged after TLP bonding.

1. Introduction

Transient liquid phase (TLP) bonding of intermetallics, including NiAl and TiAl, has been the subject of a number of investigations in recent years [1–5]. Consideration has also been given, by the authors, to the joining of intermetallic compounds to conventional metallic systems [6, 7]. In contrast, TLP bonding of dissimilar intermetallic compounds has not received a similar level of attention in the literature.

In the present paper, the authors present an investigation of the joining of martensitic NiAl (with an $L1_0$ type structure [8–10]) to martensitic NiTi (with a monoclinic structure that represents a distortion of the B19 structure [11]). Both of these martensitic intermetallics show shape-memory type behaviour [12–15] and the formation of NiAl–NiTi bonds raises the possibility of producing the shape-memory equivalent of a bi-metallic strip. NiTi martensite was chosen for investigation as this material [15] represents an important commercial shape-memory alloy (SMA). NiAl martensite was selected for study due to the existence of a baseline of information on the TLP bonding of NiAl [1–3, 6, 7, 16–18].

The authors have demonstrated previously the successful TLP bonding of (near stoichiometric) NiAl using pure copper interlayers [7]. In studies of copper-doped NiAl, the martensitic transformation is similar to that in copper-free NiAl [19]. Substitution of copper for nickel in NiTi [20–22] does not cause either significant changes to the structure of the monoclinic NiTi martensite or the formation of undesirable second-phases. Indeed, up to 25 at % of copper can be substituted for nickel in NiTi with only relatively minor changes in the martensite start (M_s) temperature [20–22]. Thus, the present investigation employed copper as an interlayer material.

Nominally stoichiometric NiTi was employed for the TLP bonds. For the NiAl substrate, a composition of Ni–24 at % Al–16 at % Cr was selected. Chromium readily forms α-Cr precipitates in Ni–(Al)–(Ti)–Cr based B2 type intermetallics [23–26] and hence is easy to detect even at low overall concentrations. Thus chromium addition to the NiAl substrate was used as a model for the transfer of ternary additions across the bond-line. For comparison, selected bonds were performed using an Ni–30 at % Al substrate with approximately the same Ni : Al ratio (2.3 : 1 for the chromium-free material versus 2.5 : 1 for the chromium-containing alloy) as the chromium-bearing substrate.

2. Experimental techniques

The NiAl/Cu/NiTi TLP bonds investigated in this paper were fabricated using the following materials:

(i) Ni–30 at % Al and Ni–24 at % Al–16 at % Cr prepared by arc melting with prior B2 grain size of around 200 μm;

(ii) Nominally stoichiometric NiTi (supplied by Shape Memory Applications, Santa Clara, CA, USA) with a grain size of around 100 μm;

0022–2461

(iii) 50 μm thick commercial purity copper (99.8% Cu) sheet.

Each substrate had a thickness of 2 mm, a faying surface area of 154 mm^2 and a 1000 grit SiC finish.

Joint fabrication was performed under a 5×10^{-4} Pa vacuum atmosphere at a bonding temperature of 1150 °C. Joints were prepared using holding times at the bonding temperature ranging from 20 min to 2 h. A heating rate of 2 °C s^{-1} and a cooling rate of 1.5 °C s^{-1} were employed.

Metallographic specimens for light microscopy (LM) and scanning electron microscopy (SEM) were prepared from the TLP bonds by electrolytic etching at 3 V in a solution comprised of 30 vol % acetic acid, 30 vol % lactic acid, 20 vol % hydrochloric acid, 10 vol % nitric acid and 10 vol % distilled water. Transmission electron microscopy (TEM) specimens were prepared by argon ion milling using dual guns operated at 5 kV with a current of 500 μA per gun and a gun to specimen angle of 13°.

TEM investigations were conducted using a JEOL 2010 instrument operated at 200 kV. SEM studies employed a JEOL 840 microscope operated at 20 kV. TEM and SEM based energy dispersive X-ray spectroscopy (EDS) investigations utilized respectively Link Isis and Tracor Northern 5500 analysers together with ultrathin window (UTW) detectors.

In this paper, the following nomenclature is used when describing TEM micrographs. Bright field images are denoted by "BF", whilst "g" is the reciprocal lattice vector of the reflection used to form a dark field (DF) image. "B" represents the beam direction of a selected area diffraction pattern (SADP). "SEI" denotes a (SEM-derived) secondary electron image.

The influence of the TLP bonding thermal cycle on the monoclinic NiTi martensite was examined using X-ray diffraction (XRD). XRD was performed, using a Rigaku diffractometer employing Cu-K_α radiation, on NiTi in the as-received condition and after 1 h at 1150 °C dummy bonding thermal cycle.

3. Results and discussion

TLP bonding in the martensitic NiAl/Cu/NiTi system was observed to occur relatively rapidly and without major changes to the martensitic NiAl substrate. In contrast, significant modification of the NiTi substrate was observed. The overall microstructural features of martensitic NiAl/Cu/NiTi TLP bonds are shown in schematic form in Fig. 1. Compositional changes with

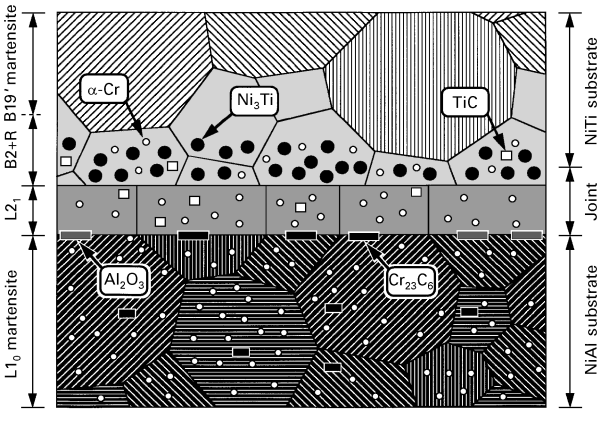

Figure 1 Schematic illustration of the main microstructural features of the martensitic NiAl/Cu/NiTi bonds.

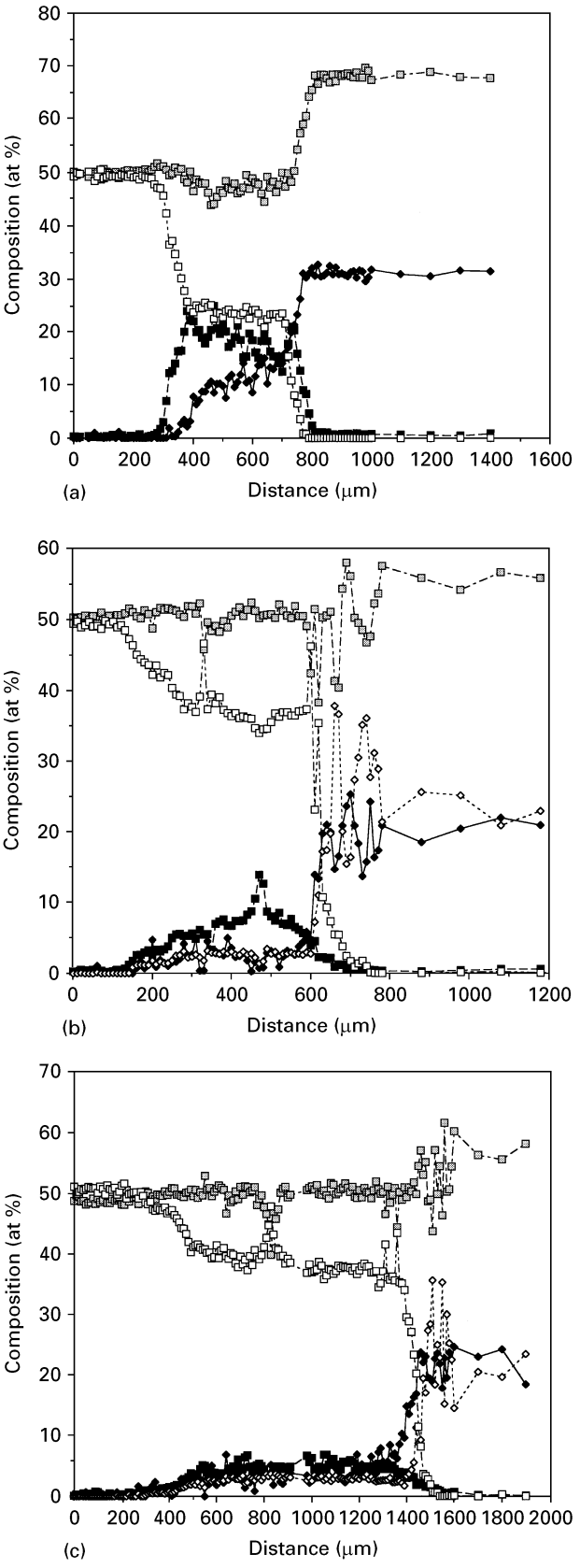

Figure 2 EDS profiles, showing changes in the composition of the martensitic NiAl/Cu/NiTi bonds with holding at the 1150°C bonding temperature: The elements are represented as: (◆) Al, (■) Cu, (◇) Cr, (▦) Ni and (□) Ti. (a) 20 min holding (chromium-free); (b) 20 min holding (chromium-doped); (c) 1 h holding (chromium-doped).

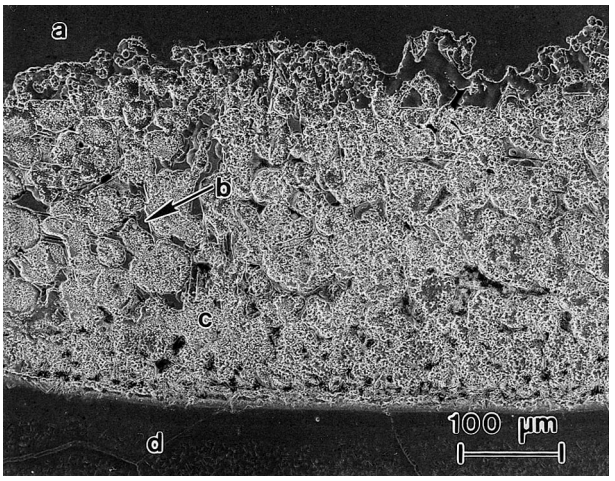

Figure 3 SEI showing the microstructure of the centre- line region of a bond held for 20 min at 1150 °C (chromium-free bond): (a = NiAl substrate; b = NiTi precipitate; c = Cu–Ni + Ni_3(Al, Ti) two phase mixture; d = NiTi substrate).

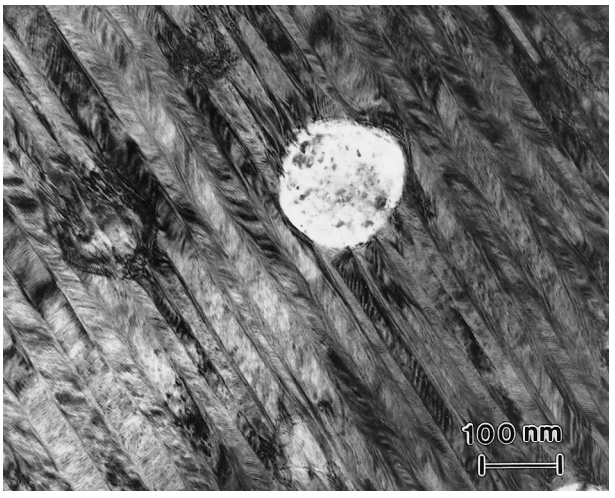

Figure 4 BF micrograph showing α-Cr precipitation in the $L1_0$ martensite matrix of the NiAl substrate in a chromium-doped bond held for 20 min at 1150 °C.

holding time at the bonding temperature are displayed in Fig. 2(a–c). Fig. 3 shows the joint microstructure prior to the completion of isothermal solidification. The microstructural features revealed in martensitic NiAl/Cu/NiTi TLP bonds will now be discussed in detail.

3.1. NiAl substrate

The microstructure of the NiAl substrate (in both the bulk substrate and adjacent to the bond-line) was dominated by the formation of internally twinned NiAl martensite with an $L1_0$ type crystal structure. This martensitic microstructure (Fig. 4) is familiar from bulk nickel-rich NiAl [8–10]. In common with the NiAl/Cu/Ni bonds previously investigated by the authors, no evidence was found for the formation of the 7R phase [27, 28] in the NiAl substrate adjacent to the bond-line. Other Ni–Al second phases, such as Ni_5Al_3 [29], were not observed. Ni_5Al_3 formation typically occurs after low-temperature ageing (e.g. 400 °C [29]), rather than at 1150 °C (as used for the TLP bonds). Thus, the absence of Ni_5Al_3 from the TLP bonds is unsurprising.

Extensive precipitation of spheroidal A2 type α-Cr (typically with a diameter of around 100 nm) was observed (Fig. 4) within the martensitic NiAl matrix. Interfacial dislocations were observed, indicating that the α-Cr formed with a semicoherent interface to the surrounding matrix. An orientation relationship was observed between the α-Cr and the $L1_0$ NiAl-martensite, such that:

$$[1\,1\,0]_{L1_0}//[0\,0\,1]_{\alpha\text{-Cr}}$$

$$(1\,\bar{1}\,1)_{L1_0}//(1\,\bar{1}\,0)_{\alpha\text{-Cr}}$$

The M_s temperature in strongly nickel enriched NiAl (e.g. 873 °C for Ni–31 at % Al [30]) is sufficiently high for chromium to retain significant mobility after the onset of the martensitic transformation. However, no evidence was found, from the distribution of α-Cr precipitates, for the heterogeneous nucleation of the α-Cr on, for example, the boundaries of the martensitic plates. Thus, the α-Cr observed within the martensitic matrix must have nucleated homogeneously and/or prior to the onset of the martensitic transformation. Given the widespread availability of heterogeneous nucleation sites within the $L1_0$ martensite and the semicoherent interface observed between the martensite and α-Cr, homogeneous nucleation of α-Cr would be expected. Thus, the formation of α-Cr in the B2 type β-NiAl phase (i.e., the parent phase in the B2 to $L1_0$ martensitic transformation), prior to the formation of the $L1_0$ martensite, will now be considered.

The orientation relationship observed in the present work, between the $L1_0$ martensite and the A2 type α-Cr, is identical to that noted previously by one of the authors between the β-NiAl phase and $L1_0$ martensite in chromium-doped nickel-rich NiAl [31]. In a number of investigations, α-Cr has been found to precipitate with a cube–cube orientation relationship to the β-phase [24–26]. Thus, α-Cr formed in advance of the martensitic transformation would be expected to show the same orientation relationship to the $L1_0$ martensite as that observed between the β-NiAl parent and $L1_0$ product of the martensitic transformation. Hence, the α-Cr–$L1_0$ orientation relationship observed in the present work is entirely consistent with the precipitation of α-Cr in the β-NiAl phase prior to the onset of the martensitic transformation.

The spheroidal α-Cr morphology and the interfacial dislocation networks observed in the present work are both characteristic of α-Cr deposits in β-NiAl [24–26]. Thus, the overall character of the α-Cr deposits was consistent with the precipitation of α-Cr in the B2 type β-NiAl phase prior to the formation of the $L1_0$ martensite. In addition to the α-Cr observed throughout the matrix of the NiAl substate, α-Cr precipitates were found on prior β–β boundaries. These precipitates showed the same orientation relationship to the $L1_0$ martensite as the other α-Cr deposits. The prior β–β boundaries were mostly low angle and so roughly the same orientation relationship was generally

established by a given α-Cr precipitate with both sides of the boundary.

Close to the bond-line, a significant build up of copper was observed in the $L1_0$ type martensitic matrix of the NiAl substrates, particularly in samples held for 1 h or longer at 1150 °C. In contrast, copper enrichment of the α-Cr precipitates was not observed, indicating that copper partitions strongly to the matrix of the NiAl substrates. Some transfer of aluminium, from the NiAl substrate to the bond-line, was also observed. However, neither this aluminium transfer, nor the copper enrichment of the NiAl substrate produced detectable changes in the microstructure of the NiAl substrate, even immediately adjacent to the bond-line.

Occasional $M_{23}X_6$ (for which M was chromium and X represented carbon) precipitates were observed within the NiAl substrates. The following orientation relationship was observed between the $M_{23}X_6$ precipitates and the $L1_0$ martensite:

$$[1\,0\,1]_{L1_0}//[0\,0\,1]_{M_{23}X_6}$$

$$(\bar{1}\,0\,1)_{L1_0}//(1\,1\,0)_{M_{23}X_6}$$

When formed intragranularly, these $M_{23}X_6$ precipitates were generally polygonal or block-like in shape with diameters typically of around 200 nm. Some $M_{23}X_6$ precipitation on prior β–β boundaries was also observed (Fig. 5a and b). Slight carbon pickup from the graphite electrode used during arc melting of the NiAl substrate material is the most likely origin of the carbon forming these $M_{23}X_6$ precipitates.

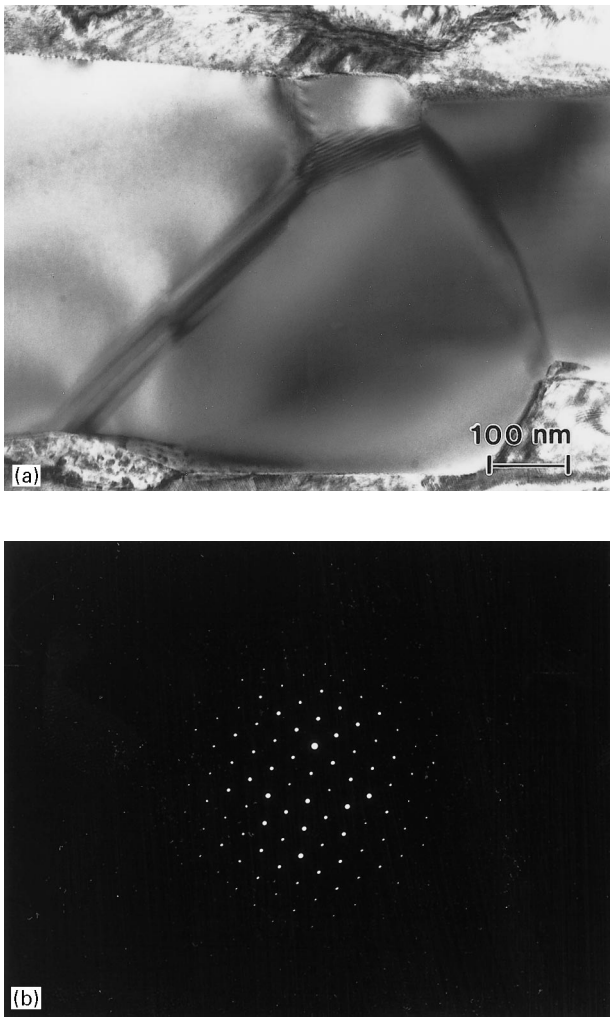

Figure 5 $M_{23}X_6$ precipitation on a (low angle) prior β–β boundary in the NiAl substrate of a chromium-doped bond held for 20 min at 1150 °C: (a) BF micrograph; (b) SADP ($B = [1\,1\,0]_{M_{23}X_6}$).

3.2. Bond-line region

In the case of solidification on-cooling, prior to the completion of isothermal solidification, the bond-line microstructure (Fig. 3) consisted of copper-rich NiTi plus two phase regions composed of $Ni_3(Al,Ti)$ precipitates in an Ni–Cu based matrix. Of rather greater interest was the microstructure formed as a result of isothermal solidification. Isothermal solidification at the bond-line was observed to proceed epitaxially from both the NiAl and NiTi substrates, with the NiTi substrate dominating the isothermal resolidification process. Given that there was no orientation relationship between the NiAl and NiTi substrates, a high angle boundary was formed within the bond-line. After 1 h at a bonding temperature of 1150 °C, isothermal solidification was complete over most of the bond-line. The only remaining liquid was at the outer regions of the samples, where slight beveling of the edges of the faying surfaces occurred during pre-bond specimen preparation leading to the collection of an excess volume of liquid during bonding.

In common with the NiAl/Cu/Ni bonds previously considered by the authors [7], some widening of the liquid seam, prior to the onset of isothermal solidification, was observed. In the NiAl/Cu/NiTi bonds, the 50 μm thick as-placed interlayer acquired a width typically of around 100 μm after 20 min holding at 1150 °C (as measured on-cooling to room-temperature). The 1 h holding time at 1150 °C required to resolidify the chromium-doped NiAl/Cu/NiTi bonds was significantly shorter than that for the NiAl/Cu/Ni bonds which required 6 h holding at 1150 °C [7]. A striking feature (Fig. 2) of the NiAl/Cu/NiTi bonds was the rapid dispersion of copper (into both the NiAl and NiTi substrates) in the case of joints made with chromium-doped NiAl, as compared with chromium-free bonds. The origins of this phenomenon remain unclear at the present time.

As was noted above, isothermal resolidification of the joints proceeded epitaxially from both the NiAl and NiTi substrates. In contrast, NiAl/Cu/Ni bonds, examined previously by the authors [7], isothermally solidified solely by growth from the NiAl substrate into the joint. This variation in isothermal solidification process may account for the difference in the time taken to complete isothermal solidification between the NiAl/Cu/Ni and NiAl/Cu/NiTi systems. In the case of resolidification proceeding from the NiTi substrate, isothermal solidification involved the growth of nickel-rich NiTi into the joint. The microstructure of this ingrowing solid was indistinguishable from that of the immediately adjacent NiTi substrate and will be discussed in the next section.

Interdiffusion between the bond-line and the NiTi substrate served to significantly modify the character

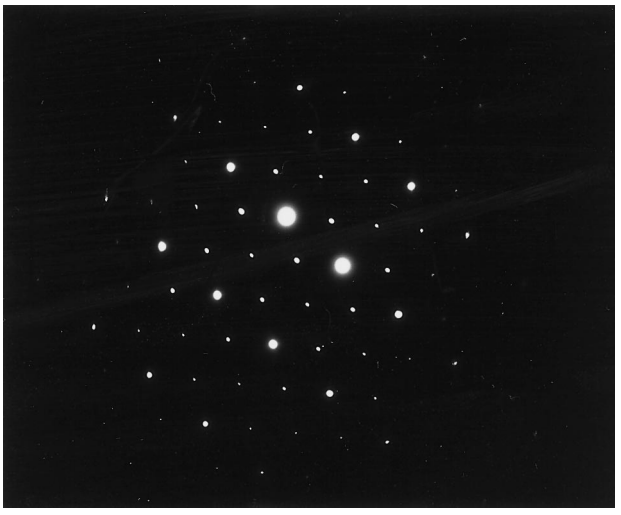

Figure 6 SADP ($B = [1\,1\,0]_{\beta'}$) showing $L2_1$ type β′ formed at the joint centre-line of a bond held for 1 h at 1150 °C.

Figure 7 BF montage showing the precipitation of $D0_{24}$ type Ni_3Ti (a) and α-Cr (b) in a B2 matrix (c) containing R-phase precipitates. The figure shows the NiTi substrate adjacent to the bond-line of a chromium-doped sample held for 1 h at 1150 °C.

of isothermal solidification proceeding from the NiAl substrate. The portion of the isothermally re-solidified joint which was epitaxial with the NiAl substrate was found to be titanium-rich when compared to the adjacent NiAl substrate. Most of this titanium-doped region was observed to have the structure (Fig. 6) and composition of the $L2_1$ type Heusler phase Ni_2AlTi (commonly known as β′). Adjacent to the NiAl substrate, the bond-line remained relatively nickel-rich, when compared to titanium, and retained a B2 structure. A cube–cube orientation relationship was observed between the β-NiAl and β′-phases, as expected, given that the $L2_1$ type β′-phase is formed by ordering of aluminium and titanium in the aluminium sublattice of the β-phase [32].

A noteworthy feature of the joint-line microstructure is the presence of the B2 phase in the joint, immediately adjacent to the $L1_0$ martensite making up the matrix of the NiAl substrate. The B2 type β-phase at the bond-line was observed to be strongly aluminium-enriched, when compared with the adjacent NiAl substrate. This aluminium-enrichment would in turn reduce the M_s temperature (for example Ni–Al alloys with aluminium contents above 38 at % have M_s temperatures below room-temperature [30]). A possible explanation of the aluminium enrichment of the bond-line B2 phase is aluminium rejection from the growing β′ phase to the joint-line β-phase.

At the interface between the NiAl substrate and the bond-line, occasional alumina precipitates and $M_{23}X_6$ carbides were observed. Presumably, these represent the remnants of the scale formed on the faying surface of the NiAl substrate during heating to the bonding temperature. Within the bond-line, the β and β′ phases contained occasional α-Cr precipitates, formed as a result of chromium transfer from the NiAl substrate to the bond-line. These α-Cr precipitates were cube–cube orientation related to the surrounding (β or β′) bond-line matrix and were in general, morphologically similar to those formed in the NiAl substrate. Occasional large (up to 1–2 μm in diameter) α-Cr precipitates were observed in the vicinity of the joint–NiAl substrate interface and these led to the serrated appearance of the compositional profiles shown in Fig. 2. The formation of a small number of TiC precipitates was observed within the bond-line region. Similar precipitates, formed in the NiTi substrate, are discussed further in the next section.

3.3. NiTi substrate

Significant modification of the NiTi substrate was observed (Fig. 7) after TLP bonding. Perhaps the most significant feature observed was the formation of a B2 type β-NiTi matrix, rather than monoclinic (with a distorted B19 structure, commonly denoted as B19′ [11]) NiTi-martensite in the vicinity of the bond-line. The formation of β-NiTi was observed after bonding for 1 h or longer at 1150 °C. The M_s temperature of NiTi is strongly sensitive to the Ni:Ti ratio and an increased extent of titanium transfer to the bond-line was observed with increased holding at 1150 °C. The resulting titanium-depletion of the NiTi substrate would, in turn, have the effect of reducing the M_s temperature to below room-temperature. Thus, after sufficient holding at 1150 °C, the β-NiTi phase would remain stable at room-temperature.

Compositional changes could conceivably be induced in the NiTi substrate by the precipitation of Ni–Ti phases, as a result of the TLP bonding thermal-cycle (as opposed to compositional changes induced by interdiffusion between the bond-line and substrate

during TLP bonding). Any such precipitation-induced compositional changes would, in turn, modify the M_s temperature of the β-NiTi phase substrate matrix. In order to determine the influence of the TLP bonding thermal cycle on the NiTi substrate, an NiTi substrate was thermally-cycled through a dummy 1 h at 1150 °C bonding treatment. The dummy TLP bonding cycle had no discernible effect on the overall structure of the NiTi substrate (as determined by XRD). Both before and after the dummy TLP cycle the NiTi substrate was found to consist largely of monoclinic NiTi-martensite with some retained B2 type β-NiTi. Thus, changes in the M_s temperature of the NiTi substrate induced directly by the TLP bonding thermal-cycle can be eliminated.

At the boundary between the bulk martensitic NiTi substrate and the β-NiTi phase region adjacent to the bond-line an additional microstructural feature was observed. The matrix of the NiTi substrate in this boundary region exhibited B2 type reflections in $\langle 111 \rangle_{B2}$ SAD patterns. In addition, weaker reflections were observed at approximately $\frac{1}{3}\{110\}_{B2}$ positions. These reflections are indicative of the formation of the "R" rhombohedral phase which is a common precursor of martensitic transformation in NiTi [11, 33].

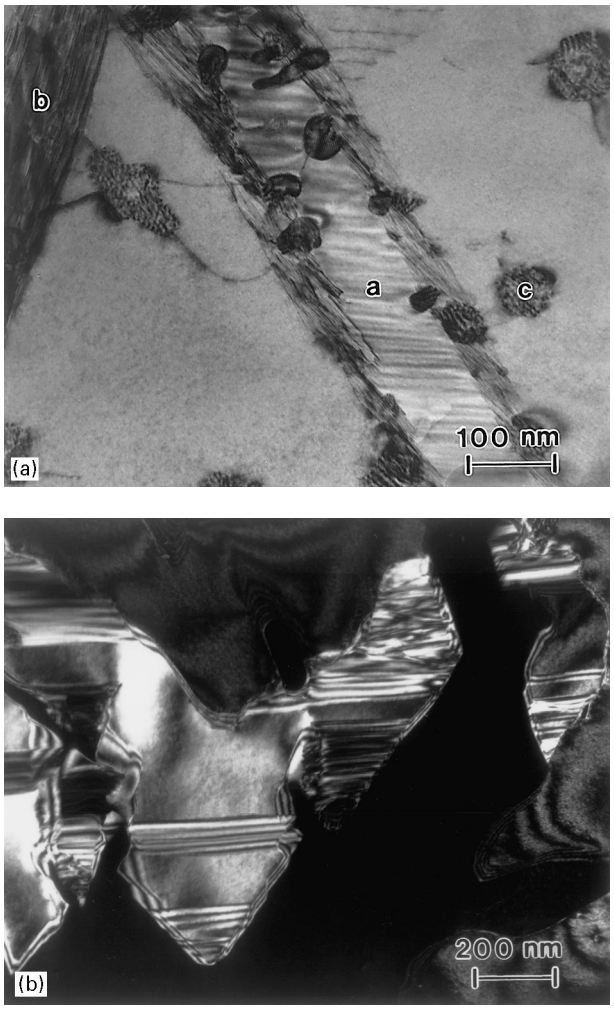

Figure 8 Precipitation of Ni_3Ti in the NiTi substrate adjacent to the bond-line of a sample held for 1 h at 1150 °C: (a) BF micrograph (a = $L1_2$ type Ni_3Ti, b = $D0_{24}$ type Ni_3Ti, c = α-Cr); (b) DF micrograph ($D0_{24}$ type Ni_3Ti light, B2 type β-NiTi dark, $\mathbf{g} = (0\,0\,0\,4)_{Ni_3Ti}$).

Within the portion of the NiTi substrate that underwent titanium-depletion during TLP bonding, extensive precipitation of Ni_3Ti was observed (Fig. 8a and b). In general, this phase was of the $D0_{24}$ type and this represents the equilibrium Ni_3Ti phase in the Ni–Ti system [34]. However, some $L1_2$ type Ni_3Ti precipitates were also observed. The $L1_2$ type γ′ phase typically has a composition $Ni_3(Al, Ti)$ and this raised the question of stabilization of the $L1_2$ structure by aluminium entering the NiTi substrate, from the NiAl substrate, via the bond-line. However, the $L1_2$ type precipitates observed in the NiTi substrate were essentially aluminium-free (indeed, relatively little aluminium was found to have entered the NiTi substrate after TLP bonding). Thus, aluminium-stabilization of the $L1_2$ can be eliminated. It is noteworthy that, in strongly nickel-rich Ni–Ti alloys, the $L1_2$ phase can appear as a metastable precipitate [35]. However, the formation of metastable $L1_2$ type Ni_3Ti in high-nickel materials presumably (at least in part) occurs as the result of the good fit between the $L1_2$ type γ′-structured phase and the A1 type Ni–Ti face centred cubic disordered solid solution. The following orientation relationship was observed between the B2 type β-NiTi phase and the $L1_2$ type Ni_3Ti:

$$[1\,1\,1]_{B2}//[1\,1\,0]_{L1_2}$$
$$(\bar{1}\,1\,0)_{B2}//(1\,\bar{1}\,\bar{1})_{L1_2}$$

whilst the orientation relationship between β-NiTi and the $D0_{24}$ type Ni_3Ti was such that:

$$[1\,1\,1]_{B2}//[1\,0\,\bar{1}\,0]_{D0_{24}}$$
$$(\bar{1}\,1\,0)_{B2}//(0\,0\,0\,1)_{D0_{24}}$$

In both cases, interfacial dislocations were observed indicating that the interfaces between the Ni_3Ti and the β-NiTi matrix were semicoherent. Thus, the origins of the formation of $L1_2$ type Ni_3Ti within the B2 regions of the NiTi substrate require further investigation.

In contrast to the formation of Ni_3Ti, other Ni–Ti second phases such as Ni_4Ti_3 or Ni_3Ti_2 were not observed. The formation of second phases other than Ni_3Ti [36–38] in the β-NiTi matrix usually involves ageing below 750 °C. However, Ni_3Ti forms directly from β-NiTi above 750 °C (even in only slightly nickel-rich materials, such as Ni–48 at % Ti). Thus, the absence of second phases other than Ni_3Ti is not surprising.

Extensive formation of α-Cr was observed within the portions of the NiTi substrate exhibiting B2 and R type crystallography. This α-Cr was cube–cube orientation related to the B2 β-NiTi phase and was usually morphologically similar to that observed in the NiAl substrate. The heterogeneous nucleation of α-Cr on β-NiTi–β-NiTi boundaries and β-NiTi–Ni_3Ti (especially $L1_2$ type) interfaces was also observed. The resulting α-Cr precipitates were often angular and dislocations punched out from these precipitates served as nucleation sites for further α-Cr.

Occasional MX type (for which M represented titanium and X carbon) precipitates were observed in the NiTi substrate immediately adjacent to the bond-line.

These precipitates were blocky and possessed the following approximate orientation relationship to the β-NiTi matrix.

$$[1\,1\,0]_{B2}//[1\,0\,0]_{MX}$$

$$(0\,0\,1)_{B2}//(0\,0\,1)_{MX}$$

In combination with occasional carbide formation throughout the NiAl substrate, the formation of TiC exclusively in the vicinity of the bond-line (and not in the bulk NiTi substrate) is compatible with entry of carbon from the NiAl substrate, via the joint, into the NiTi substrate.

In samples held for 2 h at 1150 °C, localized melting of the outer surface of the NiTi substrate, adjacent to the joint, was observed. The occurrence of this localized melting correlated with titanium depletion from the NiTi substrate by interdiffusion with the joint. Loss from the NiTi substrate of around 5 at % Ti is sufficient to reduce the solidus temperature of NiTi to 1150 °C [34]. Thus, the maximum bonding time at 1150 °C that can be employed is limited (to less than 2 h) by the need to avoid the onset of melting of the NiTi substrate. Whilst this restriction is compatible with completion of isothermal solidification, post-solidification homogenization treatments would need to be carried out at temperatures significantly below 1150 °C.

As was noted in section 4.2, a microstructural discontinuity was not observed at the interface between the NiTi substrate and the portion of the joint that underwent isothermal resolidification by epitaxial growth from the NiTi substrate. Instead, on traversing from the NiTi substrate into the joint all that was observed was a gradual increase in: (i) the copper content of the B2 β-NiTi phase, (ii) the amount of Ni_3Ti formed and (iii) the extent of precipitation of chromium and carbon-rich phases (α-Cr and TiC respectively). The solutioning of copper in nickel-rich B2 type β-NiTi has been observed previously [22]. In the present investigation, copper was found to partition strongly to the B2 phase and the formation of copper-containing second-phases was not observed.

4. Conclusions

An investigation has been undertaken of microstructural development in TLP bonds formed in the martensitic NiAl/Cu/NiTi system. As a result of this investigation, the following conclusions have been drawn:

(i) The microstructure of the NiAl substrate was largely unaffected by the TLP bonding process. However, transfer of titanium from the NiTi substrate to the bond-line had the effect of depressing the M_s temperature, of the NiTi substrate, to below room-temperature. Thus, a region of B2 type β-NiTi was produced in the NiTi substrate adjacent to the joint. This region contained both Ni_3Ti and R-type precipitates. In addition to the formation of $D0_{24}$ type Ni_3Ti, some of the Ni_3Ti precipitates were observed to adopt the $L1_2$ structure.

(ii) Isothermal solidification proceeded epitaxially from both the NiAl and NiTi substrates. Copper emanating from the joint entered solid-solution in both substrates and no evidence was found for the formation of copper-containing second-phases. Addition of chromium to the NiAl substrate appeared to hasten the isothermal solidification process. In the chromium-doped system, a 1 h hold at 1150 °C was sufficient to complete isothermal solidification. In contrast, longer holding times resulted in excessive transfer of titanium from the NiTi substrate to the joint region. Loss of titanium from the NiTi substrate, in turn, led to liquation of the outer surface of the NiTi substrate adjacent to the joint.

(iii) The progression of isothermal resolidification, from the NiAl substrate into the joint, was modified by the entry of titanium into the growing solid. The presence of significant titanium led to the formation of $L2_1$ type Ni_2AlTi in the region of the joint resolidified by epitaxial growth from the NiAl substrate. In contrast, a sudden microstructural discontinuity corresponding to the interface between the NiTi substrate and the isothermally resolidified joint was not observed.

(iv) Significant transfer of chromium from the NiAl substrate to the joint and NiTi substrate was observed, leading to the extensive precipitation of α-Cr in the NiTi substrate.

Acknowledgements

The work described in this paper was financially supported by the NSF-EPSCoR programme. TEM instrumentation employed in this research was funded by the NSF-ARI programme.

References

1. T. J. MOORE and J. M. KALINOWSKI, *MRS Symp. Proc.* **288** (1993) 1173.
2. M. J. STRUM and G. A. HENSHALL, in "*Advanced Joining Technologies for New Materials II*", edited by N. F. Flore and J. O. Stiegler (AWS, Miami, FL, 1994) p. 76.
3. W. F. GALE and S. V. OREL, *J. Mater. Sci.* **31** (1996) 345.
4. P. YAN, *Ph.D. Thesis*, University of Cambridge, Cambridge UK (1993).
5. P. YAN and E. R. WALLACH, *Intermetallics*, **1** (1993) 83.
6. W. F. GALE and S. V. OREL, *Metall. Mater. Trans. A* **27A** (1996) 1925.
7. W. F. GALE and Y. GUAN, *ibid*., in press.
8. K. ENAMI, S. NENNO and K. SHIMIZU, *Trans. JIM*. **14** (1973) 161.
9. D. SCHRYVERS, *Phil. Mag. A* **68** (1993) 1017.
10. A. S. MURTHY and E. GOO, *Acta Metall. Mater*. **41** (1993) 3435.
11. H. C. LING and R. KAPLOW, *Metall. Trans. A* **11A** (1980) 77.
12. J. A. HORTON, C. T. LIU and E. P. GEORGE, *Mater. Sci. Engng*. **A192/193** (1995) 873.
13. R. KAINUMA, K. ISHIDA and T. NISHIZAWA, *Metall. Trans. A* **23A** (1992) 1147.
14. H. A. MOHAMED and J. WASHBURN, *ibid* **7A** (1976) 1041.
15. C. M. WAYMAN, *MRS Bull.* **18**(4) (1993) 49.
16. S. V. OREL and W. F. GALE, *Schweissen Schneiden* (submitted).
17. S. V. OREL, L. PAROUS and W. F. GALE, *Weld. J.* (*Res. Suppl.*) **74** (1995) 319s.

18. *Idem*, in "Advanced Joining Technologies for New Materials II", edited by: N. F. Flore and J. O. Stiegler (AWS, Miami, FL, 1994) p. 5.
19. S.-H. KANG, S. J. JEON and H. C. LEE, *MRS Symp. Proc.* **213** (1991) 385.
20. R. H. BRICKNELL, K. N. MELTON and O. MERCIER, *Metall. Trans. A* **10A** (1979) 693.
21. R. H. BRICKNELL and K. N. MELTON, *ibid* **11A** (1980) 1541.
22. O. MERCIER and K. N. MELTON, *ibid* **10A** (1979) 387.
23. W. F. GALE, T. C. TOTEMEIER and J. E. KING, *Microstructural Sci.* **21** (1994) 61.
24. W. F. GALE and J. E. KING, *J. Mater. Sci.* **28** (1993) 4347.
25. R. YANG, J. A. LEAKE and R. W. CAHN, *Phil Mag. A* **65** (1992) 961.
26. R. D. FIELD, D. F. LAHRMAN and R. DAROLIA, *Acta Metall. Mater.* **39** (1991) 2961.
27. Y. NODA, S. M. SHAPIRO, G. SHIRANE, Y. YAMADA and L. E. TANNER, *Phys. Rev. B* **42** (1990) 10 397.
28. A. G. KHACHATURYAN, S. M. SHAPIRO and S. SEMENOVSKAYA, *ibid* **43** (1991) 10 832.
29. J. H. YANG and C. M. WAYMAN, *Intermetallics* **2** (1994) 111.
30. J. L. SMIALEK and R. H. HEHEMANN, *Metall. Trans.* **4** (1973) 1571.
31. W. F. GALE, R. V. NEMANI and J. A. HORTON, *J. Mater. Sci.* **31** (1996) 1681.
32. P. SHEN, D. GAN and C. C. LIN, *Mater. Sci. Engng.* **78** (1986) 163.
33. H. C. LING and R. KAPLOW, *Metall. Trans. A* **12A** (1981) 2101.
34. T. B. MASSALSKI (ed.), "Binary Alloy Phase Diagrams" (ASM Materials Park, OH, USA, 1986).
35. A. J. ARDELL, *Metall. Trans.* **1** (1970) 525.
36. T. TADAKI, Y. NAKATA, K. SHIMIZU and K. OTSUKA, *Trans. JIM* **27** (1986) 731.
37. M. NISHIDA, C. M. WAYMAN and T. HONMA, *Metall. Trans. A* **17A** (1986) 1505.
38. M. NISHIDA and C. M. WAYMAN, *ibid* **18A** (1987) 785.

Received 19 April
and accepted 21 May 1996